

Chapter 8

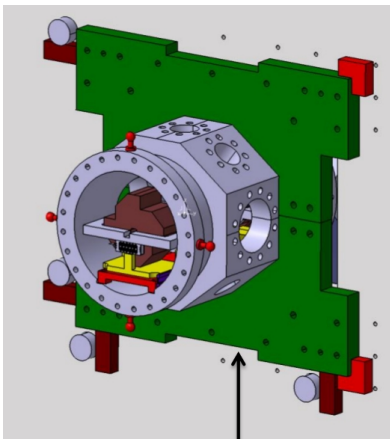
BPMS System description

In this section I describe the beam position monitor (BPM) system installed at the IP region and the signals analysis method used test the system.

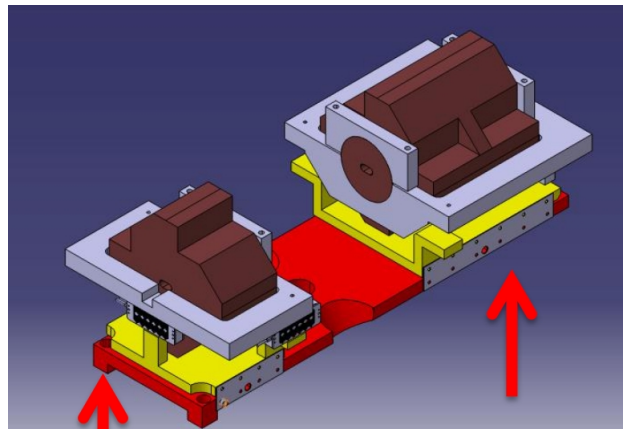
8.1 The system

The system consist in three cavities inside a vacuum chamber shown in Fig. 8.1a which is fixed to the optical table used for the IPBSM laser and optical instruments. Flanges and viewports on the sides are compatible with the IPBSM operation. Inside the chamber, a system of three cavities (IPA, IPB and IPC) are installed in two separated blocks: one block upstream for IPA and IPB and the other downstream the IP for IPC.

Each block is placed over a piezo-electric displacement system shown in Fig. 8.1b with three degrees of freedom: vertical displacement, horizontal displacement and pitch angle. Position and angle conventions can be seen in Annex B.2.



(a) Vacuum chamber design.



(b) Piezo-electric displacement system and cavities.

This piezo mover system is remotely controlled to align the cavities with the beam, and to do systematic studies of the cavity sensitivity to position change. A set of in-vacuum PT100 thermal gauges are included on each block. The initial checkings on the system can be consulted in [44], and the control and readout scheme can be seen in Annex B with alignment results.

8.1.1 The cavities

Cavities for beam position measurement show good stability since precision depends on mechanical precision. Resolution of thermal noise level can be achieved by narrowing the dynamic range and using high gain electronics since signal is small near the cavity center. The following is a description of the cavity parameters as presented by Nakamura in [45].

Cavity modes

The cavity consists of a cavity and a waveguide. When the particles pass the cavity, it resonates in several modes at frequencies given by the cavity dimension and shape [46].

Cylindrical coordinates are used for cylindrical cavities. The electric $E = (E_r, E_\phi, E_z)$ and magnetic field $B = (B_r, B_\phi, B_z)$ are excited in the cavity. For beam position monitoring TM $B = (B_r, B_\phi, 0)$ is essential. Three numbers m, n, l which are the node numbers in r, ϕ, z are used to identify the nodes. The TM_{010} is the monopole mode and it is used for charge intensity measurement and downmixing of the signals from the position sensitive cavities. It is shown in Fig. 8.3.

In a similar way, rectangular coordinates are used for rectangular cavities. The electric $E = (E_x, E_y, E_z)$ and magnetic field $B = (B_x, B_y, B_z)$ are excited in the cavity. For beam position monitoring TM $B = (B_x, B_y, 0)$ is essential. Three numbers m, n, l which are the node numbers in x, y, z are used to identify the nodes. The TM_{120} and TM_{210} are the dipole modes and are used for bunch position measurement. The TM_{110} is monopole mode in rectangular cavities. They are shown in Fig. 8.2.

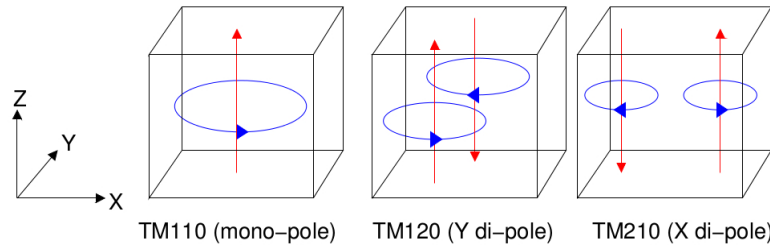


Figure 8.2 – Dipolar and monopolar mode in rectangular cavities.

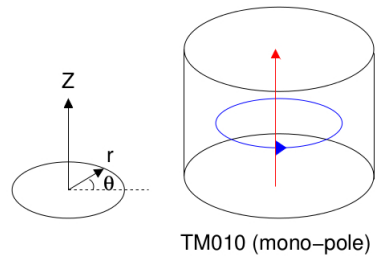


Figure 8.3 – Monopolar mode in cylindrical cavities.

Only the dipole mode is of interest for beam position measurement so it is separated from other modes which are considered noise components. The separation between the vertical and horizontal dipole mode is made by making the cavity rectangular, giving different the resonant frequencies per plane.

A set of slots is done on the cavities to couple only the dipole mode to a waveguide with a cut-off frequency above the monopole mode. This is made to separated the dipole signal from

large noise coming from the monopole component. An antenna pick-up the signal at the waveguide and connects it to the output port. The cavity design has then four ports, two ports in antiphase per plane, one on each side. Figure 8.4 shows the cavity transversal plane with the four slots and the coupling to the waveguide and the antenna for the horizontal ports.

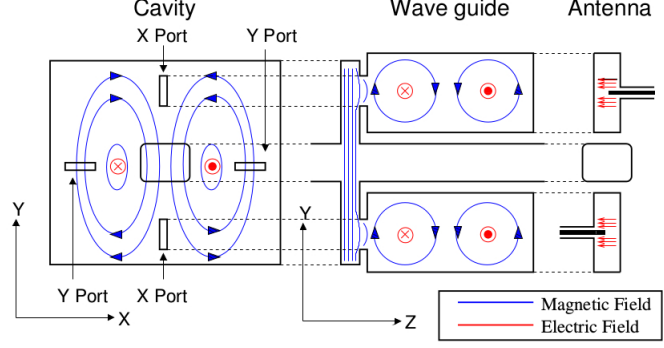


Figure 8.4 – Coupling to the dipole mode of the cavity.

Output signal

Voltage of a resonant mode excited at a cavity by passing beam, V_{exc} , is represented as

$$V_{exc} = \frac{\omega}{2} \left(\frac{R}{Q} \right) q \quad (8.1)$$

where ω is resonant angular frequency of the mode, and q is the beam charge, and R is the shunt impedance and Q is the quality factor which represents the efficiency of the resonant mode of a cavity. The factor R/Q is

$$\frac{R}{Q} = \frac{|\int E \cdot ds|^2}{\omega U} \quad (8.2)$$

where U is the energy stored in the cavity and $E \cdot ds$ is the longitudinal component of the electric field in the cavity generated by the passing beam. The cavity design for the IP region targets high R/Q (high Q_0), minimizing the energy loss in cavity walls and maximizing the output power.

The effect of bunch length σ_z is an effective reduction of V_{exc} given by the expression

$$V_{totalexc} = V_{exc} \exp \left(-\frac{\omega^2 \sigma_z^2}{c^2} \right) \quad (8.3)$$

The stored energy of a cavity is $U = V_{totalexc}^2 / (\omega R/Q)$, and the output power is $P_o = \omega U / Q_{ext}$, where Q_{ext} is the quality factor of the external coupling. Detecting the power output, P_o , by an impedance Z gives the output voltage

$$V_{out0} = \sqrt{Z P_o} = \frac{\omega q}{2} \sqrt{\frac{Z}{Q_{ext}} \frac{R}{Q}} \exp \left(-\frac{\omega^2 \sigma_z^2}{2c^2} \right) \quad (8.4)$$

The energy dissipation in the cavity is

$$U = U_0 e^{-\frac{\omega}{Q_L} t} \quad (8.5)$$

where $\frac{1}{Q_L} = \frac{1}{Q_0} + \frac{1}{Q_{ext}}$, and energy decay time $\tau = Q_L / \omega$. As the signal is proportional to the square root of the power, then the signal decay time is a factor two smaller.

Finally, as the R/Q factor depends on the longitudinal component of the electric field, the integration depends on the TM mode. It has been derived by [45] concluding that in the dipole mode R/Q depends on the square of the bunch transverse position in the case of bunch passing near the center, and the monopole mode R/Q is independent of position. From this, the output voltage in the TM₁₂₀ and TM₂₁₀ is proportional to position, while TM₁₁₀ and TM₀₁₀ are not.

Components orthogonal to position

Additional components are present in the cavity signal output which are orthogonal to bunch position. They have been described by [45] as

$$V = V_{position} + iV_{angle} + iV_{tilt} + iV_{commontail} \quad (8.6)$$

where the i shows a $\pi/2$ phase difference, and the following is a brief description of the components:

- Angle: a cavity of length L gives a position voltage as $V_{position} = Ax\sqrt{L}\sin(\omega t)$. Assuming a beam passing through the cavity center making an angle x' , it can be decomposed in the sum of two position signals with $x = x'L/4$ and phase difference of $\pm L/4c$, affecting the amplitude by $\sin(\omega L/4c)$ and phase by $\pi/2$. The ratio of angle to position signals for $\omega L/4c \ll 1$ is

$$\frac{|V_{angle}|}{|V_{pos}|} = \frac{\omega L^2}{2\sqrt{2}c} \frac{x'}{x} \quad (8.7)$$

- Tilt: a cavity gives a position voltage as $V_{position} = Aqx\sin(\omega t)$. The beam is decomposed in two point with $q/2$ total charge each, while traversing the cavity with an angle θ . The sum of two position signals with $q/2$ charge each, $x = \sigma_z\theta$ being σ_z the bunch charge, and phase difference of $\pm\sigma_z/c$ will affect the amplitude by $\theta\sigma_z^2/c$ and phase by $\pi/2$. The ratio of angle to position signals is

$$\frac{|V_{tilt}|}{|V_{pos}|} = \frac{\omega\sigma_z^2}{c} \frac{\theta}{x} \quad (8.8)$$

- Commontail: the common-tail [47] comes from the monopole component. At the dipole component frequency it is 2 to 3 orders of magnitude stronger than the dipole component. However, it is attenuated by the coupling to the waveguide. Nakamura [45] shows that the phase advance between the monopole and the dipole signals is $\pi/2$.

The phase difference of these components allow one to remove them from the position signal by phase detection. In addition the cavity design was conceived to reduce the angle signal because of the large beam divergence seen in Sect. 7.2.6.

Cavities at the IP Region

The three cavities (IPA, IPB and IPC) are rectangular and resonate in the TM₂₁₀ mode at 5.7 GHz in the horizontal plane and TM₁₂₀ at 6.4 GHz in the vertical plane. They have a design decay time of 19 ns (horizontal) and 17 ns (vertical), and sensitivities to bunch position of 2.2 $\mu\text{V}/\text{nm}/\text{nC}$ (horizontal) and 3.7 $\mu\text{V}/\text{nm}/\text{nC}$ (vertical). Two additional cylindrical cavities with decay time of 29 ns, sensitivity to bunch charge of 3.27V/nC, one per resonant frequency,

are placed downstream of the IP to measure the bunch charge and to downmix the C-Band frequency signals; these are the reference cavities.

The IPA, IPB and IPC sensitivity to orthogonal components are: position to angle ratio of $3.2 \mu\text{m}/\text{mrad}$, position to bunch tilt ratio of $8.6 \mu\text{m}/\text{mrad}$ with $\sigma_z=8 \text{ mm}$ and unknown commontail component.

Previous to the installation, the cavity signals decay time was measured giving the results shown in Table 8.1. In particular IPC shows a shorter signal than IPA and IPB. The effect of the large difference between the design and the measured values on resolution is under investigation.

Plane	Design	IPA	IPB	IPC
X [ns]	19.41	8.722	8.181	4.925
Y [ns]	17.49	11.11	11.25	6.745

Table 8.1 – Measured decay time for the three cavities before installation.

The measured resonant dipole frequency and the design show good agreement in Table 8.2.

Plane	Design	Average	IPA	IPB	IPC
X [MHz]	5712	5712	-2	-2.5	+2.5
Y [MHz]	6426	6420	+1	0	-3.5

Table 8.2 – Resonant dipole frequency measurement at KEK before installation.

8.1.2 The processing electronics

Each position measurement cavity has two output ports in antiphase per plane connected to independent processing electronics to downmix the signals, separate them into two orthogonal components called I and Q , and set the gain according to beam charge conditions. A set of remotely-controllable attenuators, variable between 0-70 dB in steps of 10 dB is used to increase the linear range of electronics at the expense of resolution.

At the moment the reference cavities are not used to downmix the position cavities signals directly to base band. Instead a 714 MHz signal from the DR is used to downmix the three to 714 MHz in a first stage and then a second stage downmixes the position cavities to baseband using the reference cavity signal. This allows the installation of the second stage outside the ATF2 line, aiming the study of the signal with different phase detection setting changed by hand in hardware. An scheme of the electronics is in Fig. 8.5. The following is a description of components extracted from [45].

- Combiner: The combiner outputs the difference of the signals. However, the signal from the two cavity ports are in antiphase so the net effect is factor 2 of amplification.
- Variable attenuator: it attenuates the input signal from 0 dB to 70 dB in steps of 10 dB. The purpose is to enlarge dynamic range at the expense of resolution.
- First stage of down conversion: it downmixes the BPM and reference cavity signals to 714 MHz using an $8 \times 714 \text{ MHz}$ signal from the LOCKED LO module, and amplifies the output by 20 dB. It is required to do it as close as possible to the BPMs because of the short decay time.

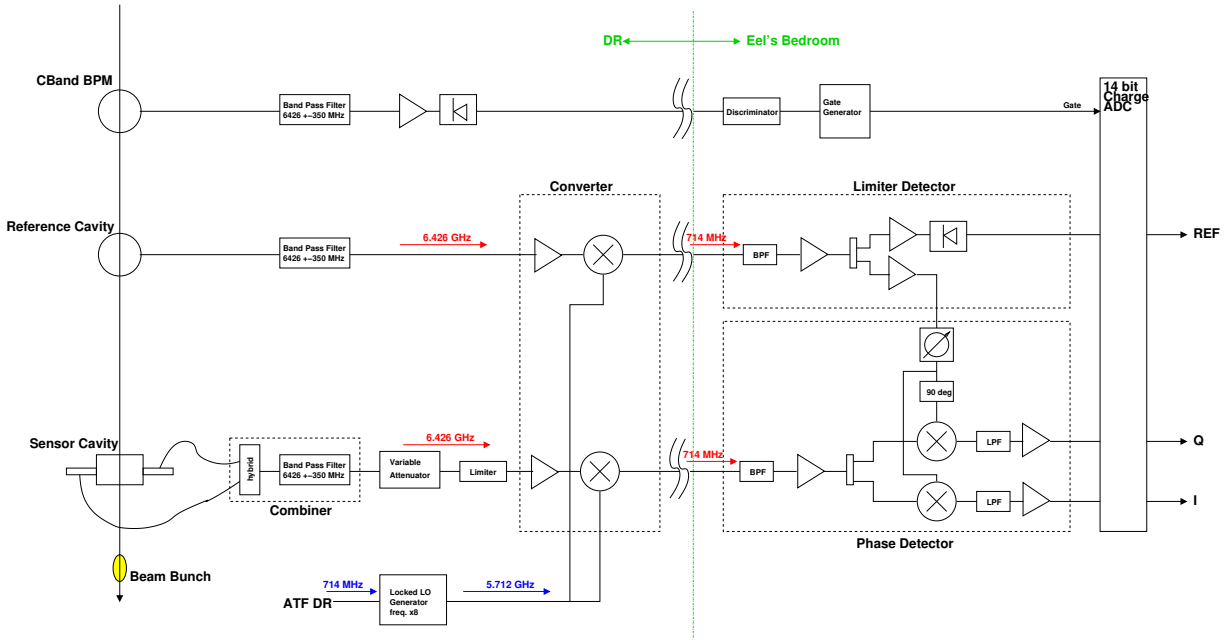


Figure 8.5 – Processing electronics per BPM per plane.

- **LOCKED LO:** Multiplies the frequency of the DR 714 MHz by a factor 8 to perform the first stage of signal downmixing.
- **Limiter detector:** Set a constant amplitude of the Reference signal at 714 MHz to be used for the downmixing in the second stage. Fig. 8.6 shows a diagram with 4 outputs to be used for downmixing. It also outputs the signal proportional to charge.
- **Phase detector:** It sets the common phase between the ref cavity signal and the IPBPMs signals by means of a knob. Then, it separates the IPBPMs signals in two set of orthogonal components by downmixing the signals at 0° , 90° , 45° and 135° . The outputs at 0° and 90° are amplified by 25 to 30 dB, and the 45° and 135° outputs by extra 10 dB according to the module used. One of the two orthogonal sets is read as *I* and *Q*.

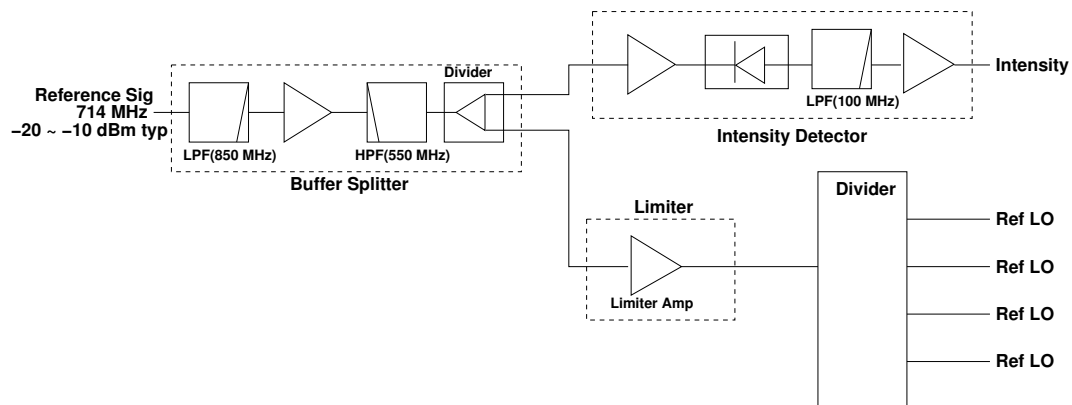


Figure 8.6 – Limiter detector.

At the moment only one Limiter detector is available, therefore, only the acquisition of only four signals was possible. Priority was given to the study of the three IPBPMs vertical signals. The horizontal signals were studied only for alignment matters.

The noise floor of the first stage of downmixing has been previously measured to be -95 dBm ($4 \mu V_{rms}$). It limits the resolution to 2 to 3 nm (horizontal) and 1 to 2 nm (vertical) at 0.5×10^{10} particles per bunch because of sensitivities shown in Sect. 8.1.1.

The gain and attenuation setting are used to get the maximum of the dynamic range within the acquisition system limits in Sect. 8.1.4. The dynamic range of the electronics is estimated as follows: at 10 dB attenuation, 0.4×10^{10} particles and $3.7 \mu C/nm/nC$ vertical position sensitivity the signal is $0.75 \mu V/nm$. This signal is amplified by a total of 53.7 dB from the first (+20 dB) and second (+43.7 dB) downmixing stages with 10 dB losses estimation from cables and couplers. Using +2.5 V of the acquisition range, the signal dynamic range is $6.9 \mu m$. This can be directly compared with the dynamic range measurement in Sect. 9.2.

However, the first downmixing stage specifications show a typical input value of -60 dBm ($223.7 \mu V_{rms}$). It imposes a tighter limit on the dynamic range of 300 nm. The estimated input signal to the first downmixing stage and $6.9 \mu m$ offset is -33 dB ($5 mV_{rms}$).

8.1.3 Feedback system

A local beam-based feedback system has been installed at the IP, in order to stabilise the beam position at the IP. This system comprises a stripline kicker, just upstream of the IP chamber, a fast kicker amplifier and digital feedback controller, and can be driven by any of the three IPBPM IQ signals, or a linear combination of the signals from any two BPMs. The system is designed for operation on a bunch train of two or more bunches, separated by less than 150-200 ns, where the measurement of first bunch provides the input to the feedback system, and the correction is applied to subsequent bunches.

8.1.4 The acquisition system

The acquisition system samples the two downmixed orthogonal waveforms per cavity per plane over the decay time. This amounts to 14 simultaneous channels: I and Q waveforms for both x and y for each of the three position measurement cavities plus the charge signal from each of the two reference cavities.

The resolution required to measure 1 nm over the $10 \mu m$ of dynamic range is at least 14 bits (2^{14} discrete steps). However, several systems have been used along the IPBPM operation.

Initially a set of four Agilent 3000 X-Series oscilloscopes of 8 bits resolution, four channels each, $5V_{rms}$ dynamic range and up to 4 Gsamples/s was used for IPBPMs commissioning. Also a dedicated acquisition board, FONT5, operated by FONT group to perform the IP feedback was used. It digitised 9 channels synchronized in banks of three, 13 bits resolution, and a maximum sampling of 400 MHz with ± 0.5 V dynamic range.

A dedicated acquisition system built around an SIS digitizer has recently been introduced. The resolution is 14-bits, the dynamic range is either 2 or 5 V, and the sampling frequency is configurable with 238 MHz being the typical value. This is an important step towards integration of the IP position measurements into the existing ATF control system.

8.2 BPM Analysis Method

The system has been tested with three sets of optics : (1) parallel beam (large beam size at waist and hence approximately constant beam size through the IP region) (2) nominal and (3)

low beta.

The longitudinal position of the beam focus was moved closer to the location of IPB, by changing the strength of the FD, to reduce the beam jitter at IPB, allowing operation without additional attenuation and hence maximal sensitivity.

8.2.1 Waveform analysis

The I and Q waveforms are analysed by choosing a single sample on the signal. In general, the on-peak sample is chosen except in cases where the post analysis shows saturation of the processing electronics. The identification of position I' and orthogonal components Q' requires a position scan.

Averaging or integrating the samples may do little to improve the analysis due to the presence of (714 ± 10) MHz band pass filters between the first and second stage of downmixing of the processing electronics as part of an investigation into the reduction of large unwanted static waveform components.

8.2.2 Position scans

While the beam is running the cavity position is systematically changed and the I and Q waveforms are acquired and analysed offline to obtain the signal change to displacement ratio, known as calibration factor.

By definition I' is position signal and Q' are orthogonal signals to position. Figure 8.7 shows that the systematic change I' signal could change the I and Q values because of a relative phase fixed by the detector between the reference and the IQ signals. In addition, the mismatch between the BPMs dipole frequencies with respect to the reference cavity frequency generates a constant rotation of the I and Q signals from sample to sample.

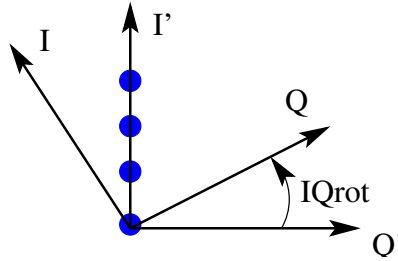


Figure 8.7 – IQ rotation. The blue dots represent the systematic change in position.

The position scan analysis allows to identify I' and Q' by the following procedure:

- Single samples in the waveform for I , Q and Ref signals are chosen.
- The I and Q values per pulse are divided by the Ref value, in order to remove the charge dependence. We have now I_n and Q_n .
- Plotting I_n vs Q_n allows one to find the IQ rotation angle, IQ_{rot} .
- The I_n and Q_n are counter rotated by the IQ_{rot} angle, finding I' and Q' .

The ratio $I'/\Delta y$ in a.u./ μm is the cavity calibration factor, C_{bpm} .

It also gives the information of the beam center position, $I' = 0$, and the amplitude in μ of the constant orthogonal component Q'/C_{bpm} .

8.2.3 Angle scans

First a position scan should be done to identify I' and Q' signal. Then, a combination of piezo-movers setting keep the cavity center stable and changes the BPM pitch angle in systematic steps while the beam is running. See Appendix B.2.2 for the movers settings.

The I and Q signals are analysed applying the IQ_{rot} angle from the position scan, and it will show the change in I' and Q' while changing the angle. The Q'/θ_p and the calibration factor from the position scan are divided to find the angle to position ratio. It has been measured for IPBy giving $3.2 \mu m/mrad$ as expected from cavity parameters [48].

8.2.4 Jitter acquisitions

The beam jitter is determined from measurement of the bunch position over several hundred pulses with a static BPM mover setting.

Consider now the signal S as the sum of the two outputs from the cavity. The signal S for the vertical outputs of one BPM and one bunch is composed of:

$$S = y + is_p\theta_p + s_{xy}(x + is_y\theta_y) + x\theta_r \quad (8.9)$$

where i indicates $\pi/2$ phase difference. s_p is the sensitivity to pitch angle, s_{xy} is the inverse of X-Y isolation, s_y is the yaw angle sensitivity. $x, y, \theta_p, \theta_r, \theta_y$, are horizontal position, vertical position, pitch, roll and yaw angles BPM with respect to beam.

Signal S can be separated in real and imaginary parts:

$$S = (y + s_{xy}x + x\theta_r) + i(s_p\theta_p + s_{xy}s_y\theta_y) \quad (8.10)$$

The amplitud $|S|$ is the total contribution to signal and should be then below the dynamic range of the first downmixing stage.

This signals are rotatated by an arbitrary angle ϕ to obtain the I' and Q' at the phase shifter block.

$$\begin{aligned} S &= \underbrace{(y + s_{xy}x + x\theta_r)(\cos \phi + i \sin \phi)}_{I'} + \underbrace{i(s_p\theta_p + s_{xy}s_y\theta_y)(\cos \phi + i \sin \phi)}_{Q'} \\ &= I' + Q' \end{aligned}$$

In the case of perfect IQ rotation ($\phi = 0$), all imaginary (angle and others) component is removed from real (position) component in the S signal. However, in practice this rotation could be achieved to precision set by $\Delta\phi$, then, to first order

$$S = [(y + s_{xy}x + x\theta_r) - \Delta\phi(s_p\theta_p + s_{xy}s_y\theta_y)] + i[\Delta\phi(y + s_{xy}x + x\theta_r) + (s_p\theta_p + s_{xy}s_y\theta_y)] \quad (8.11)$$

At this point onw will be only interested in the real part as it contains most of the vertical position signal.

$$\Re[S] = S_y = (y + s_{xy}x + x\theta_r) - \Delta\phi(s_p\theta_p + s_{xy}s_y\theta_y) \quad (8.12)$$

The last equation shows the contribution to vertical signal from the relative position BPM to beam.

Mean value of S_y signal over m bunches sample will be equal to

$$\langle S_y \rangle = [y_0 + (x_0 + \eta\delta)(s_{xy} + \theta_{r0})] - \Delta\phi[s_p\theta_{p0} + s_{xy}s_y(\theta_{y0} + \eta'\delta)] \quad (8.13)$$

where all 0-index correspond to misalignment, η and η' are the dispersion and dispersion angle optic parameters, $\delta = 10^{-3}$ is the energy spread, and no beam rotation is considered. The alignment purpose is to make $\langle S \rangle = 0$.

The signal jitter $\sigma_{S_y}^2 = \langle S_y^2 \rangle - \langle S_y \rangle^2$ will come from

$$\begin{aligned}\sigma_{S_y}^2 &= \sigma_{jy}^2 + \sigma_{jx}^2 [s_{xy} + \theta_{r0}]^2 + (\Delta\phi)^2 [s_p^2 \sigma_{jy'}^2 + s_{xy}^2 s_y^2 \sigma_{jx'}^2] \\ &= \langle y^2 \rangle - y_0^2 + (\langle x^2 \rangle - x_0^2) [s_{xy} + \theta_{r0}]^2 + (\Delta\phi)^2 [s_p^2 (\langle y'^2 \rangle - y_0'^2 + s_{xy}^2 s_y^2 (\langle x'^2 \rangle - x_0'^2))]\end{aligned}$$

and subtracting all means effects

$$\sigma_{S_y}^2 = \langle y^2 \rangle + \langle x^2 \rangle [s_{xy} + \theta_{r0}]^2 + (\Delta\phi)^2 [s_p^2 \langle y'^2 \rangle + s_{xy}^2 s_y^2 \langle x'^2 \rangle] \quad (8.14)$$

Isolation X-Y ($1/s_{xy}$) was measured to be under 50dB ($\text{Pin/Pout} < 10^{-5} = 3.162 \times 10^{-3}$ voltage isolation), sensitivity to pitch (s_p) was measured to be $3.2\mu\text{m/mrad}$, and sensitivity to yaw (s_y) is $2.9\mu\text{m/mrad}$ estimated in similar way to s_p .

For 1 nm contribution to beam size we get:

$$1 \text{ nm} \geq \sqrt{\langle x^2 \rangle} [s_{xy} + \theta_{r0}] = \sqrt{\langle x^2 \rangle} [1.880 \times 10^{-3} + \theta_{r0}] \quad (8.15)$$

$$1 \text{ nm} \geq \Delta\phi s_p \sqrt{\langle y'^2 \rangle} = 3.2\Delta\phi \sqrt{\langle y'^2 \rangle} \quad (8.16)$$

$$1 \text{ nm} \geq \Delta\phi s_{xy} s_y \sqrt{\langle x'^2 \rangle} = 5.453 \times 10^{-3} \Delta\phi \sqrt{\langle x'^2 \rangle} \quad (8.17)$$

where the BPM vertical ($3.7\text{mV}/\mu\text{m/nC}$) and horizontal ($2.2\text{mV}/\mu\text{m/nC}$) sensitivities have been used to translate voltage isolation X-Y to position scale, position jitter is in nm and angle jitter in μrad .

Tables 8.3-8.6 show the jitters at the beam waist and the furthest BPM IPA for the two optics with the largest angular jitters.

Jitter	10%	20%
$\sigma_{yj}(\text{nm})$	3	7
$\sigma_{xj}(\text{nm})$	283	565
$\sigma_{y'j}(\mu\text{rad})$	34	69
$\sigma_{x'j}(\mu\text{rad})$	71	141

Table 8.3 – Jitter at beam waist with 1BX1BY optics.

Jitter	10%	20%
$\sigma_{yj}(\text{nm})$	3	7
$\sigma_{xj}(\text{nm})$	894	1787
$\sigma_{y'j}(\mu\text{rad})$	34	69
$\sigma_{x'j}(\mu\text{rad})$	22	44

Table 8.4 – Jitter at beam waist with 10BX1BY optics.

Using the jitters at beam waist with the 10BX1BY optics one can obtain $\theta_{r0} \leq 0.6 \text{ mrad}$ and $|\Delta\phi| \leq 4.525 \text{ mrad}$ are required to 1 nm resolution.

The current precision of $|\Delta\phi|$ has been found to be 43 mrad by redoing 7 calibrations one after another. This is 10 times bigger than the specified and could contribute to 3 to 4 nm.

Jitter	10%	20%
$\sigma_{yj}(\text{nm})$	5766	11531
$\sigma_{xj}(\text{nm})$	11866	23733
$\sigma_{y'j}(\mu\text{rad})$	0	0
$\sigma_{x'j}(\mu\text{rad})$	1	3

Table 8.5 – Jitter at IP with 1BX1BY optics.

Jitter	10%	20%
$\sigma_{yj}(\text{nm})$	5766	11531
$\sigma_{xj}(\text{nm})$	3856	7713
$\sigma_{y'j}(\mu\text{rad})$	0	0
$\sigma_{x'j}(\mu\text{rad})$	5	10

Table 8.6 – Jitter at IPA with 10BX1BY optics.